Journal of Computational Physics **163,** 452–466 (2000)
doi:10.1006/jcph.2000.6576, available online at http://www.idealibrary.com on IDEAL

Free Vibration Analysis of Curvilinear Quadrilateral Plates by the Differential Quadrature Method

C. Shu,* W. Chen,* and H. Du†

Department of Mechanical and Production Engineering, National University of Singapore, 10 Kent Ridge Crescent, Singapore 119260; and †School of Mechanical and Production Engineering, Nanyang Technological University, Nanyang Avenue, Singapore 639798

Received June 15, 2000; revised June 22, 2000

A methodology for applying the differential quadrature (DQ) method to the free vibration analysis of arbitrary quadrilateral plates is developed. In our approach, the irregular physical domain is transformed into a rectangular domain in the computational space. The governing equation and the boundary conditions are also transformed into relevant forms in the computational space. Then all the computations are based on the computational domain. As compared to the approach proposed by C. W. Bert and M. Malik (*Int. J. Mech. Sci.* **38**, 589 (1996)), the present approach requires much less computational effort and virtual storage. In addition, the present work uses a simple and convenient way to implement clamped and simply supported boundary conditions. An exact mapping technique is used to perform the coordinate transformation in this study. Some numerical examples are provided to show the computational efficiency of the present scheme. © 2000 Academic Press

Key Words: differential quadrature method; vibration analysis; arbitrary quadrilateral plates; coordinate transformation.

INTRODUCTION

In recent years, the differential quadrature (DQ) method has become increasingly popular in the numerical solution of initial and boundary value problems [1]. The advantages of the DQ method lie in its easy use and flexibility with regard to arbitrary grid spacing. Compared to the conventional low-order numerical techniques such as the finite element and finite difference methods, the DQ method can yield accurate solutions with relatively much fewer grid points. On the other hand, it is well known that the strength of the finite element method is its ability to handle irregular geometry with curved boundaries. In previous applications, the DQ method was limited to distributed parameter systems or problems with regular domains. Recent studies have extended the application of the DQ method in

0021-9991/00 $35.00

solving relatively complex problems. Shu [2] presented a DQ multidomain approach to fluid mechanics problems with irregular domains. Lam [3] introduced a mapping technique to apply the DQ method to conduction, torsion, and heat flow problems with arbitrary geometries. These applications involved the second-order differential systems. Striz *et al.* [4] and Wang and Gu [5] developed two different schemes for a DQ element to analyze some realistic structural problems with discontinuous loads or geometry. Bert and Malik [6] made the first attempt to apply the DQ method to the vibration analysis of irregular plates. Liew and Han [7, 8] also used a similar approach to analyze irregular quadrilateral thick plates. All these efforts show that the element and mapping techniques can extend the DQ method to general geometry problems while retaining its attractive features of rapid convergence and high accuracy.

The contribution of Bert and Malik [6] is that they were the first to handle curvilinear geometries involving structural mechanics problems in fourth-order differential systems. The difficulties of the high-order systems lie in the complexity of the governing and boundary equations. In Bert and Malik's approach, the matrices of the first-order derivatives in the x and y directions are first formed by the DQ method. Then by using the differential chain rule and matrix multiplication techniques, the matrices for the discretization of the higher-order derivatives are obtained. It is noted that the idea of Bert and Malik's approach is very simple. However, the computational effort and virtual storage required by Bert and Malik's approach are very large. Actually, the dimension of the matrix by matrix multiplication in Bert and Malik's approach is $(N_x N_y) \times (N_x N_y)$, which is much larger than $(N_x \times N_x)$ used in the regular domain. Here, N_x and N_y represent the numbers of grid points along the x and y directions. Therefore, the computational effort for a matrix multiplication is proportional to the order of $(N_x N_y)^4$ scalar multiplications. In contrast, the traditional DQ application to two-dimensional problems with regular domains only involves on the order of $(N_x N_y)^2$ scalar multiplications. Therefore, Bert and Malik's approach requires much larger computational effort in comparison to the application of DQ to regular domain problems, especially for a large number of grid points.

The boundary condition equations used by Bert and Malik [6] involve the angle between the normal to the plate boundary and the x axis. When applied to problems with complex curvilinear boundaries, this may increase the programming and computing effort by having to obtain the value of the angle at each boundary point. Another problem in Bert and Malik's approach is that cubic serendipity shape functions are used to map plate configurations having curvilinear edges. As pointed out by Campion and Jarvis [9], geometric mapping is more demanding for a large element, which is often employed in high-order or global numerical techniques such as the DQ method. In some cases, the cubic serendipity shape functions are sufficiently accurate for mapping the irregular domain into a square region. However, for complex geometries, it is necessary to employ more accurate mapping techniques [10].

This paper focuses on the DQ vibration analysis of irregular plates. Some innovations are presented to cure the above-mentioned deficiencies in Bert and Malik's approach. First, we derive the governing and boundary condition equations of a vibrating plate in the curvilinear coordinate system (computational space). By using these equations, the conventional differential quadrature rule on the rectangular domain can be directly extended to handle the complex geometry problems. Therefore, only the original DQ weighting coefficients in each direction are involved, and the procedure of the reformation of the quadrature rules in Bert and Malik [6] is no longer needed. Second, an approach is presented to implement the boundary conditions, which does not involve the angle between the normal to the plate boundary and the x axis. The implementation of this approach is very simple, especially for the simply supported condition. Third, following the approach proposed by Shu and Du [11, 12], two boundary conditions at each boundary are exactly satisfied in the present study while, in contrast, only one boundary condition is exactly satisfied at the δ-technique implemented by Bert and Malik [6]. Therefore, the drawbacks of the δ-technique are eliminated. Another improvement in the present work is to employ exact mapping for the coordinate transformation. Exact geometric mapping circumvents the effects of the inaccuracies of the mapping on the DQ solutions. Finally, some numerical examples are provided to demonstrate the computational efficiency of the present approach.

2. DIFFERENTIAL QUADRATURE METHOD

One of the key issues in the DQ method is how to determine its weighting coefficients. The earlier approach, which required solving algebraic equations with an ill-conditioned Vandermonde matrix, is neither efficient nor accurate when the number of grid points is large [13]. By using the analysis of a high-order polynomial approximation and of a linear vector space, Shu and Richards [13] presented a simple algebraic formulation or a recurrence relationship to compute the weighting coefficients of the DQ method. For the nth-order derivative of a function $f(x, t)$ with respect to x at a grid point x_i, the DQ approximation can be expressed as

$$f_x^{(n)}(x_i, t) = \sum_{k=1}^{N} c_{ik}^{(n)} \cdot f(x_k, t), \quad n = 1, 2, \ldots, N-1, \quad i = 1, 2 \ldots, N, \tag{1}$$

where N is the number of grid points in the whole domain and $c_{ik}^{(n)}$ are the weighting coefficients to be determined by the DQ method. As shown in the work of Shu and Richards [2] and Shu and co-workers [11–14], the weighting coefficients of the first-order derivative can be calculated by a simple algebraic formulation without any restriction on the choice of grid point distribution, and the weighting coefficients of the second- and higher-order derivatives can be computed from a recurrence relationship. For details of these computations, the reader is advised to refer to Refs. [2, 11–14].

3. COORDINATE TRANSFORMATION FROM PHYSICAL SPACE TO COMPUTATIONAL SPACE

Like low-order finite difference schemes, the DQ method requires the computational domain to be rectangular. For irregular domains, the DQ method cannot be applied directly. To apply the DQ method to such problems, a coordinate transformation is necessary; that is, the irregular physical domain is transformed into a regular computational domain. An example of coordinate transformation is shown in Fig. 1. The coordinate transformation can be made using the expression

$$x = x(\xi, \eta) \tag{2a}$$

$$y = y(\xi, \eta). \tag{2b}$$

It is noted that Eq. (2) gives a one-to-one mapping from the physical space (x, y) to the computational space (ξ, η) or from the computational space (ξ, η) to the physical space (x, y).

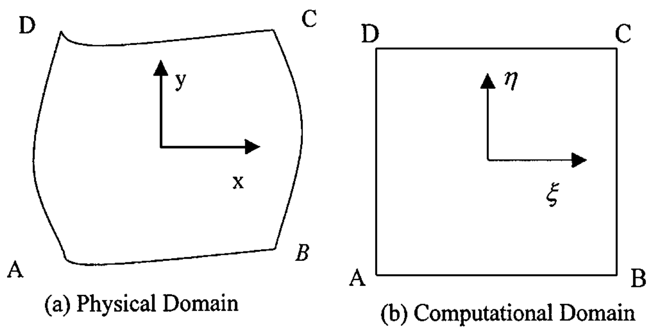

FIG. 1. Physical and computational domains.

In the work of Bert and Malik [6], $x(\xi, \eta)$ and $y(\xi, \eta)$ are taken as the isoparametric shape functions used in the finite element analysis. However, since the computational domain of the DQ method is much larger than that of finite elements, this kind of transformation may cause significant errors when the domain is large and any of the boundaries has a high curvature. To improve this, accurate transformation expressions are needed. The blending function method is such a scheme, which was originated in a computer-aided design [15] and used by Malik and Bert [20] in the DQ application. In this study, we will introduce this technique for coordinate transformation.

Several kinds of blending functions are available. Defining the vector $V(\xi, \eta)$ as

$$V(\xi, \eta) = \begin{bmatrix} x(\xi, \eta) \\ y(\xi, \eta) \end{bmatrix},$$

the linear blending function gives [15]

$$\begin{aligned} V(\xi, \eta) = {} & \left(\frac{1-\xi}{2}\right) M(-1, \eta) + \left(\frac{1+\xi}{2}\right) M(1, \eta) + \left(\frac{1-\eta}{2}\right) M(\xi, 1) \\ & + \left(\frac{1+\eta}{2}\right) M(\xi, 1) - \frac{(1-\xi)(1-\eta)}{4} M(-1, -1) - \frac{(1-\xi)(1+\eta)}{4} M(-1, 1) \\ & - \frac{(1+\xi)(1-\eta)}{4} M(1, -1) - \frac{(1+\xi)(1+\eta)}{4} M(1, 1), \end{aligned} \tag{3}$$

where the functions $M(\xi_i, \eta)$ and $M(\xi, \eta_j)$ represent the four boundary parametric curves of the original physical domain and the function $M(\xi_i, \eta_j)$ denotes the x and y coordinates of the point corresponding to the coordinates (ξ_i, η_j) in the computational space.

For the geometry shown in Fig. 2, Eq. (3) gives

$$x(\xi, \eta) = [r_d + (a - r_d)(\eta + 1)/2] \cos(\varphi(\xi + 1)/2), \tag{4a}$$

$$y(\xi, \eta) = [r_d + (a - r_d)(\eta + 1)/2] \sin(\varphi(\xi + 1)/2), \tag{4b}$$

where

$$r_d = \frac{\sin(\pi - \alpha - \varphi\xi/2)}{\sin(\varphi\xi/2)} b,$$

$$\alpha = -\arcsin\left[\frac{e}{b} \sin(\varphi\xi/2)\right],$$

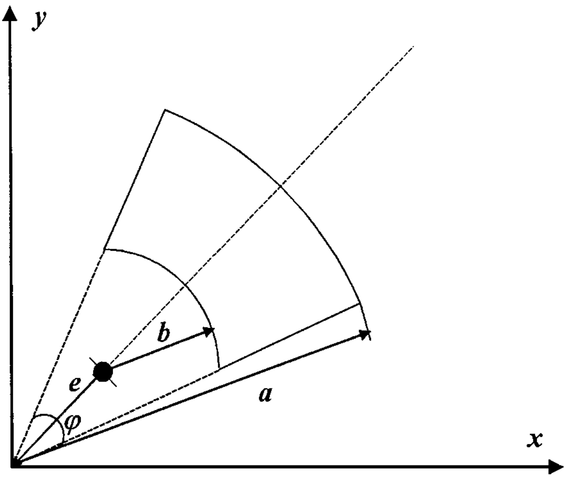

FIG. 2. An eccentric sectorial plate.

φ is the angle of the sectorial plate, a is the radius of the outer surface, b is the radius of the inner surface, and e is the distance between two centers of eccentric surfaces. For the geometry shown in Fig. 3, Eq. (3) is simplified to

$$x(\xi,\eta) = a(\xi+1)/2, \tag{5a}$$

$$y(\xi,\eta) = -\sqrt{b^2-(b^2-c^2)(\xi+1)/2} + 2\eta\sqrt{b^2-(b^2-c^2)(\xi+1)/2}. \tag{5b}$$

Similarly, using Eq. (3), we have

$$x(\xi,\eta) = 0.75(1+\eta) + 0.25(1+\eta)\cos\left(\frac{\pi}{8}-\frac{\pi}{8}\xi\right), \tag{6a}$$

$$y(\xi,\eta) = 0.375(1-\xi)(1+\eta) + 0.25(1-\eta)\sin\left(\frac{\pi}{8}-\frac{\pi}{8}\xi\right) \tag{6b}$$

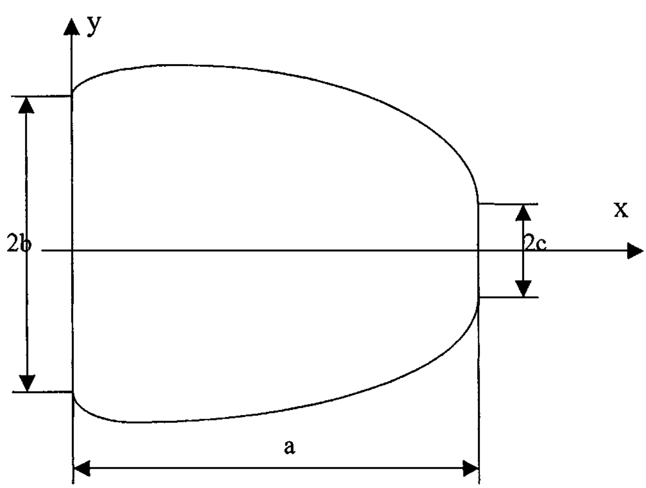

FIG. 3. A symmetric, parabolic, trapezoidal plate.

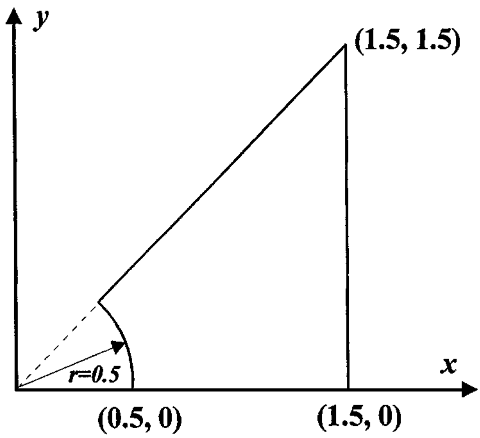

FIG. 4. A section of a right triangular plate with a corner cutout.

for the geometry shown in Fig. 4 and

$$x(\xi, \eta) = (0.6255\eta + 2.6255)\cos((\xi + 1)\pi/4), \tag{7a}$$

$$y(\xi, \eta) = (0.87551\eta + 1.8755)\sin((\xi + 1)\pi/4) \tag{7b}$$

for the geometry shown in Fig. 5. It is indicated that Bert and Malik [6], using a cubic shape function, have also considered the geometries shown in Figs. 2 and 3. All of the above geometries will be used as test examples for the present study.

4. PLATE VIBRATION EQUATIONS IN THE CURVILINEAR COORDINATE SYSTEM

In this section, we will show the plate vibration equations in the curvilinear coordinate system so that the traditional DQ rules for regular domains [11] can be directly extended to the plate vibration problems with arbitrary quadrilateral domains. The equation governing

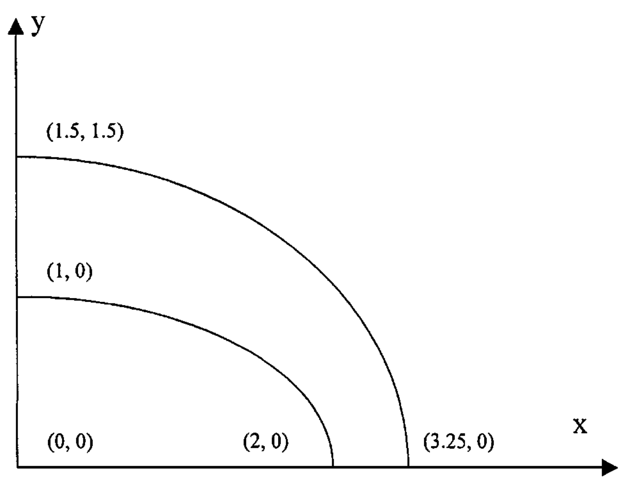

FIG. 5. A quarter section of an elliptical plate.

the free vibration of plates can be expressed as

$$w_{xxxx} + 2w_{xxyy} + w_{yyyy} = \Omega^2 w, \tag{8}$$

where $\Omega = \omega a^2\sqrt{\rho h/D}$, D is the plate stiffness, h is the total plate thickness, ρ is the density, w is the deflection, and ω is the natural frequency of free vibration. The governing equation (8) can be transformed in the (ξ, η) system (computational space) into the form

$$\begin{aligned}
&\bar{D}^{(41)} w_{,\xi\xi\xi\xi} + \bar{D}^{(42)} w_{,\xi\xi\xi\eta} + \bar{D}^{(43)} w_{,\xi\xi\eta\eta} + \bar{D}^{(44)} w_{,\xi\eta\eta\eta} + \bar{D}^{(45)} w_{,\eta\eta\eta\eta} + \bar{D}^{(31)} w_{,\xi\xi\xi} \\
&\quad + \bar{D}^{(32)} w_{,\xi\xi\eta} + \bar{D}^{(33)} w_{,\xi\eta\eta} + \bar{D}^{(34)} w_{,\eta\eta\eta} + \bar{D}^{(21)} w_{,\xi\xi} + \bar{D}^{(22)} w_{,\xi\eta} \\
&\quad + \bar{D}^{(23)} w_{,\eta\eta} + \bar{D}^{(11)} w_{,\xi} + \bar{D}^{(12)} w_{,\eta} = \Omega^2 w,
\end{aligned} \tag{9}$$

where

$$\begin{aligned}
\bar{D}^{(41)} &= a^2, \\
\bar{D}^{(42)} &= 2ab, \\
\bar{D}^{(43)} &= 2ac + b^2, \\
\bar{D}^{(44)} &= 2cb, \\
\bar{D}^{(45)} &= c^2, \\
\bar{D}^{(31)} &= 2da + 2aa_\xi + ba_\eta, \\
\bar{D}^{(32)} &= 2bd + 2ae + 2ab_\xi + 2ca_\eta + ba_\xi + bb_\eta, \\
\bar{D}^{(33)} &= 2dc + 2ac_\xi + 2be + 2cb_\eta + bb_\xi + bc_\eta, \\
\bar{D}^{(34)} &= 2ec + 2cc_\eta + bc_\xi, \\
\bar{D}^{(21)} &= d^2 + 2ad_\xi + da_\xi + ea_\eta + aa_{\xi\xi} + ba_{\xi\eta} + ca_{\eta\eta} + bd_\eta, \\
\bar{D}^{(22)} &= 2de + 2ae_\xi + 2cd_\eta + db_\xi + bd_\xi + eb_\eta + be_\eta + ab_{\xi\xi} + bb_{\xi\eta} + cb_{\eta\eta}, \\
\bar{D}^{(23)} &= e^2 + 2ce_\eta + dc_\xi + ec_\eta + ac_{\xi\xi} + bc_{\xi\eta} + cc_{\eta\eta} + be_\xi, \\
\bar{D}^{(11)} &= dd_\xi + ed_\eta + ad_{\xi\xi} + bd_{\xi\eta} + cd_{\eta\eta}, \\
\bar{D}^{(12)} &= de_\xi + ee_\eta + ae_{\xi\xi} + be_{\xi\eta} + ce_{\eta\eta},
\end{aligned}$$

$$a = \frac{A}{J}, \quad b = \frac{2B}{J}, \quad c = \frac{C}{J}, \quad d = \frac{(A_\xi + B_\eta)}{J}, \quad e = \frac{(B_\xi + C_\eta)}{J},$$

$$A = \frac{\alpha}{J}, \quad B = \frac{-\beta}{J}, \quad C = \frac{\gamma}{J},$$

$$\alpha = x_\eta^2 + y_\eta^2, \quad \beta = x_\xi x_\eta + y_\xi y_\eta, \quad \gamma = x_\xi^2 + y_\xi^2, \quad J = x_\xi y_\eta - x_\eta y_\xi.$$

The variable domain of Eq. (9) is a rectangle as shown in Fig. 1. It is noted that Eq. (9) with varying coefficients $\bar{D}^{(ij)}$ is much more complicated in form than Eq. (8). However, it should be indicated that, since the computational domain is regular, Eq. (9) can be solved in exactly the same way as regular domain problems by using the DQ method.

Simply supported (SS) and clamped (C) boundary conditions will be considered in the present study. They are given as follows:

Clamped (C)

$$w = 0, \tag{10a}$$

$$\frac{\partial w}{\partial n} = 0. \tag{10b}$$

Simply Supported (SS)

$$w = 0, \tag{11a}$$

$$\frac{\partial^2 w}{\partial n^2} + \nu \frac{\partial^2 w}{\partial \tau^2} = 0, \tag{11b}$$

where n and τ denote the normal and tangential directions, respectively. Equations (10a) and (11a) represent zero deflection, Eq. (10b) represents zero normal rotation, and Eq. (11b) represents zero normal moment. The zero deflection condition can be easily implemented. In the work of Bert and Malik [6], the zero normal rotation and moment conditions in the clamped and simply supported edges are expressed as

$$w_{,x} \cos\theta + w_{,y} \sin\theta = 0, \tag{12}$$

$$(\cos^2\theta + \nu \sin^2\theta) w_{,xx} + (\sin^2\theta + \nu \cos^2\theta) w_{,yy} + 2(1-\nu)\cos\theta \sin\theta w_{,xy} = 0, \tag{13}$$

where θ is the angle between the normal to the plate boundary and the x-axis. It is noted that Eq. (12) is equivalent to Eq. (10b), while Eq. (13) is equivalent to Eq. (11b). In the following, we will show how to simplify Eqs. (12) and (13) along the ξ = constant and η = constant boundaries in the curvilinear coordinate system.

For the clamped and simply supported edges, the deflection w is always zero. Thus, we have

$$\frac{\partial w}{\partial \eta} = 0 \tag{14a}$$

$$\frac{\partial^2 w}{\partial \eta^2} = 0 \tag{14b}$$

on the ξ = constant boundaries, and

$$\frac{\partial w}{\partial \xi} = 0 \tag{15a}$$

$$\frac{\partial^2 w}{\partial \xi^2} = 0 \tag{15b}$$

on the η = constant boundaries. On the other hand, we note that θ is the angle between the normal to the plate boundary and the x axis. So, along the ξ = constant boundaries, we have

$$\cos\theta = y_\eta / \sqrt{\alpha} \tag{16a}$$

$$\sin\theta = -x_\eta / \sqrt{\alpha}. \tag{16b}$$

Using Eqs. (14) and (16), the zero normal rotation condition (12) along the ξ = constant boundaries can be simplified to

$$\frac{\partial w}{\partial \xi} = 0 \tag{17}$$

and the zero normal moment condition (13) along the ξ = constant boundaries can be reduced to

$$\frac{\partial^2 w}{\partial \xi^2} - \frac{2\beta}{\alpha}\frac{\partial^2 w}{\partial \xi \partial \eta} + s\frac{\partial w}{\partial \xi} = 0, \tag{18}$$

where

$$s = \frac{1}{J\alpha^2}[(\alpha^2 y_{\xi\xi} - 2\alpha\beta y_{\xi\eta} + \beta^2 y_{\eta\eta})x_\eta - (\alpha^2 x_{\xi\xi} - 2\alpha\beta x_{\xi\eta} + \beta^2 x_{\eta\eta})y_\eta] + \frac{\nu J}{\alpha^2}(y_{\eta\eta}x_\eta - x_{\eta\eta}y_\eta).$$

Similarly, along the η = constant boundaries, $\cos\theta$ and $\sin\theta$ can be expressed as

$$\cos\theta = y_\xi/\sqrt{\gamma} \tag{19a}$$

$$\sin\theta = -x_\xi/\sqrt{\gamma}. \tag{19b}$$

Therefore, Eq. (12) is reduced to

$$\frac{\partial w}{\partial \eta} = 0 \tag{20}$$

and Eq. (13) is simplified to

$$\frac{\partial^2 w}{\partial \eta^2} - \frac{2\beta}{\gamma}\frac{\partial^2 w}{\partial \xi \partial \eta} + t\frac{\partial w}{\partial \eta} = 0, \tag{21}$$

where

$$t = \frac{1}{J\gamma^2}[(\beta^2 x_{\xi\xi} - 2\gamma\beta x_{\xi\eta} + \gamma^2 x_{\eta\eta})y_\xi - (\beta^2 y_{\xi\xi} - 2\gamma\beta y_{\xi\eta} + \gamma^2 y_{\eta\eta})x_\xi] + \frac{\nu J}{\gamma^2}(x_{\eta\eta}y_\xi - y_{\eta\eta}x_\xi).$$

5. APPLICATIONS AND DISCUSSIONS

In this section, the DQ method is used to solve Eq. (9) governing the transverse vibration of irregular plates. The independent variables ξ and η in the square computational domain as shown in Fig. 1 range from -1 to 1. Application of the DQ method to Eq. (9) gives

$$\begin{aligned}&\bar{D}_{ij}^{(41)} D_{ik}^{\xi} w_{kj} + \bar{D}_{ij}^{(42)} C_{ik}^{\xi} A_{jm}^{\eta} w_{km} + \bar{D}_{ij}^{(43)} B_{ik}^{\xi} B_{jm}^{\eta} w_{km} + \bar{D}_{ij}^{(44)} A_{ik}^{\xi} C_{jm}^{\eta} w_{km} + \bar{D}_{ij}^{(45)} D_{jm}^{\eta} w_{im}\\ &+ \bar{D}_{ij}^{(31)} C_{ik}^{\xi} w_{kj} + \bar{D}_{ij}^{(32)} B_{ik}^{\xi} A_{jm}^{\eta} w_{km} + \bar{D}_{ij}^{(33)} A_{ik}^{\xi} B_{jm}^{\eta} w_{km} + \bar{D}_{ij}^{(34)} C_{jm}^{\eta} w_{im} + \bar{D}_{ij}^{(21)} B_{ik}^{\xi} w_{kj}\\ &+ \bar{D}_{ij}^{(22)} A_{ik}^{\xi} A_{jm}^{\eta} w_{km} + \bar{D}_{ij}^{(23)} B_{jm}^{\eta} w_{im} + \bar{D}_{ij}^{(11)} A_{ik}^{\xi} w_{kj} + \bar{D}_{ij}^{(12)} A_{jm}^{\eta} w_{im} = \Omega^2 w_{i,j}\end{aligned} \tag{22}$$

for $i, j = 3, \ldots, (N-2)$, where A_{ij}, B_{ij}, C_{ij}, and D_{ij} with superscripts ξ and η denote the weighting coefficient matrices of the first-, second-, third-, and fourth-order derivatives along the ξ and η directions, and N and M are the numbers of grid points along the ξ and η directions, respectively. The repeated index k means summation from 1 to N along the ξ direction, while the repeated index m indicates summation from 1 to M along the η direction. It is noted that all the DQ weighting coefficient matrices in Eq. (22) are obtained in the same way as the application of the DQ method to regular domain problems. It is noted that Eq. (22) only involves the order of N^2M^2 scalar multiplications.

Because vibration plate problems are actually high-order boundary value problems with double boundary conditions at each edge, some careful consideration is needed to properly implement the boundary conditions [11, 12]. To our knowledge, at least four kinds of approaches are available to implement such multiple boundary conditions. The earliest is the so-called δ-technique proposed by Bert *et al.* [16] and widely used in the literature. The approach enforces the geometric boundary conditions at the actual boundary points and the derivative boundary conditions at the δ points, which are a very small distance δ ($\delta \cong 10^{-5}$ in dimensionless values [6]) away from the respective boundary. Thus, one boundary condition cannot be satisfied exactly at the boundary points and the accuracy of the solutions is affected. As mentioned earlier, arbitrariness in the choice of the δ value may introduce unexpected oscillations into the solution behavior. To overcome the drawbacks of the δ approach, Wang and Bert [18] developed a new technique which incorporates the boundary conditions into the DQ weighting coefficient matrices in advance, and then the weighting coefficients with built-in boundary conditions are employed to discretize the governing equations for the problems of interests. The essence of the approach is that the boundary conditions are applied during the formulation of the weighting coefficient matrices for the inner grid points. The technique improves the accuracy of the DQ solution for problems with simply supported conditions. However, the technique is limited to simple problems due to its inability to handle problems with discontinuous geometry and loading as well as cross derivative boundary conditions. Chen *et al.* [21] presented an efficient approach to treat the fourth-order boundary conditions. More recently, Wang and Gu [5] presented a so-called differential quadrature element method (DQEM). The DQEM shows flexibility in a variety of beam and beam structure problems with discontinuous geometry and loading. However, it also seems to have difficulty in covering problems with mixed partial derivative boundary conditions. An intuitive methodology is to directly implement the double boundary conditions exactly at the edge points. Shu and Du [11, 12] showed a systematic use of the methodology in the solution of vibration problems for beams and plates with various boundary conditions, including the first application to plates with free corners. The approach of Shu and Du is conceptually simple and effective for all types of boundary conditions. The idea of this approach is to replace the discretized governing equation by the discretized boundary condition equation for some interior points.

According to the above discussion, one can easily conclude that only the conventional δ-technique and Shu and Du's approach are capable of solving problems with cross derivative boundary conditions encountered in irregular geometry problems. It is well demonstrated in [11, 12] that the accuracy, simplicity, efficiency, and stability of Shu and Du's approach are consistently superior to those of the δ-technique. Therefore, in this study we adopt Shu and Du's approach to implement double boundary conditions at each edge.

In the present study, the mesh point distribution used in the work of Shu and Richards [13] is adopted to generate the mesh points in the computational space. The algorithm is

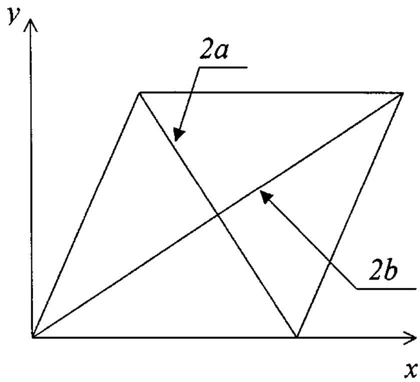

FIG. 6. A rhombic plate.

carried out in FORTRAN 77 and is run on a HP C200 workstation using double precision arithmetic. The performance of the present method is demonstrated through the vibration solution of plates with irregular geometry as shown in Figs. 2–6. Table I displays the first six frequencies of the flexural vibration of eccentric sectorial plates. The DQ results are obtained using a mesh size of 21×21 for three cases of the SS–SS–SS–SS, SS–C–SS–C, and C–C–C–C configurations. It can be seen from the table that the present DQ results agree very well with those given by Bert and Malik [6]. It should be pointed out that the differences between the present solutions and those in Bert and Malik [6] are due to the use of different approaches for coordinate transformation and implementation of multiple boundary conditions. Figure 7 shows the ratio of CPU time (present/reference [6]) versus N (the number of grid points in the x direction) for the vibration analysis of eccentric sectorial plates. It is noted that the CPU time of Ref. [6] is also obtained on a HP C200. We edited a program using the approach proposed in Ref. [6] and ran it on a HP C200. In this study, the numbers of grid points used in the x and y directions are taken to be the same. It is apparent that for the same number of grid points, solution by the present method requires much less CPU time than solution by Bert and Malik's approach. It should be pointed out that the computational effort in the solution of the resulting eigenvalue equation system

TABLE I

Converged Solutions of the First Six Frequencies of Flexural Vibration of Eccentric Sectorial Plates (Fig. 2: $a/b = 8/3$, $e/b = 1.0$, $\varphi = 45°$, $\Omega = \omega a^2/\pi^2\sqrt{\rho h/D}$)

	Mode					
$N = M$	1	2	3	4	5	6
			SS–SS–SS–SS			
21	17.717	23.168	33.744	48.564	62.542	65.863
[6]	17.592	23.130	33.729	48.575	62.414	65.878
			SS–C–SS–C			
21	35.361	37.727	45.998	58.537	75.918	93.540
[6]	35.352	37.794	46.010	58.560	75.941	93.721
			C–C–C–C			
21	36.405	40.417	50.487	65.448	85.239	95.720
[6]	36.360	40.452	50.498	65.463	85.254	95.782

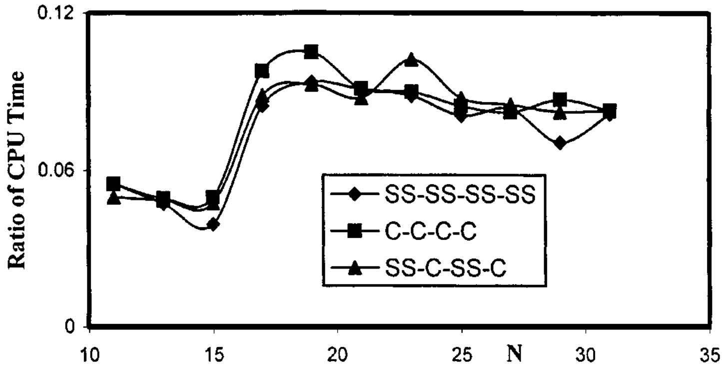

FIG. 7. Ratio of CPU time (present/reference [6]) versus N ($=M$) for vibration analysis of eccentric sectorial plates.

is the same in the present approach and Bert and Malik's approach. The computational efficiency of the present approach comes from the fact that it does not involve on the order of N^4M^4 scalar multiplications to obtain the discretization matrices for higher-order derivatives. It was found from Fig. 7 that the solution of the resultant eigenvalue equation system dominates the CPU time in the present approach, while, in contrast, the operation of matrix multiplication accounts for most of the CPU time in Bert and Malik's approach. On the other hand, by comparing solutions for plates with different boundary conditions, it is seen that CPU time does not change much when the same number of grid points is used.

The results of the first six frequencies of flexural vibration of symmetric parabolic trapezoidal plates with C–C–C–C, SS–C–SS–C, and C–SS–C–SS boundaries are presented in Table II. It is noted that there is a small difference between the present solutions and those in Bert and Malik [6] due to the different implementation of the coordinate transformation

TABLE II

Converged Solutions of the First Six Frequencies of Flexural Vibration of Symmetric Parabolic Trapezoidal Plates (Fig. 3: a/b = 3.0, b/c = 2.5; $\Omega = \omega a^2/\pi^2\sqrt{\rho h/D}$)

	Mode					
$N = M$	1	2	3	4	5	6
			C–C–C–C			
17	9.3723	13.9641	19.7460	21.8375	27.2672	29.1650
[6]	9.3645	13.977	19.799	21.843	27.334	29.139
PV-2 Ritz[a]	9.3428	14.1186	20.0527	21.6208	27.6616	29.2138
			SS–C–SS–C			
17	8.5709	12.8800	18.0984	20.7258	24.6152	27.7824
[6]	8.5694	12.886	18.154	20.746	24.691	27.757
			C–SS–C–SS			
19	5.4742	9.9289	15.4196	16.1466	21.930	24.2740
[6]	5.4831	9.9535	15.424	16.178	21.942	24.306

[a] The solutions of the PV-2 Ritz method were provided by Mr. Yang Lei of the Civil Engineering Department of National University of Singapore.

TABLE III
Converged Solutions of the First Six Frequencies of Flexural Vibration of a Right Triangular Plate with a Corner Cutout (Fig. 4: $\Omega = \omega a^2\sqrt{\rho h/D}$)

	Mode					
$N = M$	1	2	3	4	5	6
			SS–SS–SS–SS			
21	1.226	2.655	3.259	4.462	5.655	6.119
			SS–C–SS–C			
19	1.526	3.068	3.707	4.978	6.243	6.696
			C–C–C–C			
19	2.362	4.198	4.928	6.416	7.771	8.308

and the boundary conditions. Solutions of a C–C–C–C plate using the PV-2 Ritz method are also included in Table II. It is observed that the DQ solutions agree very well with those yielded by the PV-2 Ritz method. It should be indicated that in the case of symmetric parabolic trapezoidal plates with all edges simply supported, the present approach has faster convergence speed using unequal numbers of grid points than using equal numbers of grid points along the ξ and η directions. This coincides with Bert and Malik's approach. For the sake of brevity, we do not display the relative solutions here.

The vibration of irregular plates as shown in Figs. 4 and 5 was also investigated. To the authors' knowledge, such plate configurations have never been analyzed before. Therefore, these results are provided as benchmarks for future research. Both the present and Bert and Malik's approaches are applied to solve these problems. It was found that the two results were almost the same. Table III summarizes the first six frequencies of flexural vibration of a right triangular plate with a corner cutout. Since the results of Bert and Malik's approach are almost the same as those of present approach, only the present results are shown in Table III. In Table IV, the DQ solutions of the first six frequencies of flexural vibration of an elliptical sectorial plate are given. It is noteworthy that the present DQ solutions obtained with a mesh size of 11×11 are very accurate. This may be due to less mapping distortion being present. It is true for all the cases that grid distortion caused by geometric mapping impairs the accuracy of the DQ method compared with that of DQ solutions of regular domain problems.

TABLE IV
Converged Solutions of the First Six Frequencies of Flexural Vibration of Quarter Sections of Elliptical Plates (Fig. 5: $\Omega = \omega a^2\sqrt{\rho h/D}$)

	Mode					
$N = M$	1	2	3	4	5	6
			SS–SS–SS–SS			
11	0.491	0.773	1.183	1.624	1.699	1.997
			C–SS–C–SS			
11	0.536	0.879	1.358	1.675	1.943	2.178
			C–C–C–C			
11	0.974	1.292	1.715	2.245	2.444	2.980

TABLE V
Converged Solutions of the First 10 Frequencies of Flexural Vibration of Clamped Rhombic Plate (Fig. 6: $\Omega = \omega a^2\sqrt{\rho h/D}$)

	Mode									
$N = M$	1	2	3	4	5	6	7	8	9	10
17	12.703	23.369	28.254	34.738	45.948	48.969	49.794	61.130	65.361	74.533
[6]	12.703	23.369	—	34.738	45.948	48.969	49.794	61.130	65.362	74.535
[19]	12.70	23.37	28.25	34.74	45.95	48.98	49.79	61.13	—	74.54

Finally, Table V lists the first 10 frequencies of clamped rhombic plates when the ratio of the major and minor diagonal lengths (b/a) is 1.5 : 1. The geometry of these plates is shown in Fig. 6. For this case, Bert and Malik [6] could not converge on the third frequency. This may be due to the fact that one of the double boundary conditions at each edge is imposed at the so-called δ point in their approach, which is not exactly on the boundary. It is claimed [6] that Gorman [19] gave the most accurate solutions of this case by using the superposition method. The present DQ solutions agree very well with those given by Gorman [19]. It is also interesting to note that Gorman [19] did not provide the ninth frequency for this problem.

6. CONCLUSIONS

This paper presents a new approach to the study of the vibration of irregular plates with simply supported and clamped boundary conditions. In this approach, the irregular physical domain is transformed into a regular domain (square) in a curvilinear coordinate system (computational space) and, accordingly, the governing equation and boundary conditions are transformed into relevant forms in the curvilinear coordinate system. Then all computations are based on the computational domain. Since the computational domain is regular, the application of the DQ method to irregular plates in the computational space is exactly the same as the application of the DQ method to regular plates in the physical domain. The only difference is that more terms are involved in the governing equation and the boundary conditions in the curvilinear coordinate system. The present approach avoids the huge operation of matrix multiplication, which is involved in Bert and Malik's approach [6], and, as a result, computational effort and virtual storage are greatly reduced. It is demonstrated through test examples that the present approach requires less than one-tenth of the CPU time that Bert and Malik's approach requires when the number of grid points is the same. In addition, the present paper introduces a simple way to implement the simply supported and clamped boundary conditions, which avoids the difficulty of determining the angle between the direction normal to the boundary and the x axis used in Bert and Malik's approach. An exact coordinate transformation is used in the present work, and the two boundary conditions at each edge are satisfied accurately at the boundary points. It is demonstrated by test examples that, although the present approach requires less CPU time than Bert and Malik's approach, it shows slight improvement in the accuracy of the numerical results as compared to Bert and Malik's approach. This improvement is probably due to the use of an exact coordinate transformation in the present work and to the different implementation of the boundary conditions between the two approaches. Through the present study, it can be concluded that the present approach combines the attractive features of rapid convergence and high accuracy of the DQ solution of regular domain problems with general geometric flexibility. This work makes the DQ method more promising for further development into an efficient and flexible numerical technique for solving practical engineering problems.

REFERENCES

1. C. W. Bert and M. Malik, Differential quadrature method in computational mechanics: A review, *Appl. Mech. Rev.* **49**, 1 (1996).
2. C. Shu and B. E. Richards, Parallel simulation of incompressible viscous flows by generalized differential quadrature, *Comput. Syst. Eng.* **3**, 271 (1992).
3. S. S. E. Lam, Application of the differential quadrature method to two-dimensional problems with arbitrary geometry, *Comput. Struct.* **47**, 459 (1993).
4. A. G. Striz, Weilong Chen, and C. W. Bert, Static analysis of structures by the quadrature element method (QEM), *Int. J. Solids Struct.* **31**, 2807 (1994).
5. X. Wang and H. Gu, Static analysis of frame structures by the differential quadrature element method, *Int. J. Numer. Methods Eng.* **40**, 759 (1997).
6. C. W. Bert and M. Malik, The differential quadrature method for irregular domains and applications to plate vibration, *Int. J. Mech. Sci.* **38**, 589 (1996).
7. K. M. Liew and J. Han, A four-node differential quadrature method for straight-sided quadrilateral Reissner/Mindlin plates, *Commun. Numer. Methods Eng.* **13**, 73 (1997).
8. J. Han and K. M. Liew, An eight-node curvilinear differential quadrature formulation for Reissner/Mindlin plates, *Comp. Methods Appl. Mech. Eng.* **141**, 265 (1997).
9. S. D. Campion and J. L. Jarvis, An investigation of the implementation of the p-version finite element method, *Finite Elements Anal. Design* **23**, 1 (1996).
10. O. C. Zienkiewicz, *The Finite Element Method*, 3rd ed. (London: McGraw–Hill, 1973).
11. C. Shu and H. Du, Implementation of clamped and simply supported boundary conditions in the GDQ free vibration analysis of beams and plates, *Int. J. Solids Struct.* **34**, 819 (1997).
12. C. Shu and H. Du, A generalized approach for implementing general boundary conditions in the GDQ free vibration analysis of plates, *Int. J. Solids Struct.* **34**, 837 (1997).
13. C. Shu and B. E. Richards, Application of generalized differential quadrature to solve two-dimensional incompressible Navier–Stokes equations, *Int. J. Num. Methods Fluids* **15**, 791 (1992).
14. C. Shu and Y. T. Chew, On the equivalence of generalized differential quadrature and highest order finite difference scheme, *Comput. Methods Appl. Mech. Eng.* **155**, 249 (1998).
15. W. J. Gordon, Blending-function methods of bivariate and multivariate interpolation and approximation, *SIAM J. Numer. Anal.* **8**, 158 (1971).
16. C. W. Bert, S. K. Jang, and A. G. Striz, Two new approximate methods for analyzing free vibration of structural components, *AIAA J.* **26**, 612 (1988).
17. J. F. Thompson, Z. U. A. Warsi, and C. W. Mastin, *Numerical Grid Generation: Foundation and Applications* (Elsevier/North–Holland, New York, 1985).
18. X. Wang and C. W. Bert, A new approach in applying differential quadrature to static and free vibrational analyses of beams and plates, *J. Sound Vibration* **62**, 566 (1993).
19. D. J. Gorman, Accurate free vibration analysis of Rhombic plates with simplysupported and fully-clamped edge conditions, *J. Sound Vibration* **125**, 281 (1988).
20. M. Malik and C. W. Bert, Differential quadrature analysis for curvilinear domains via geometric mapping by blending functions, in *Applied Mechanics in the Americas (PACAM V, San Juan Puerto Rico), 1997*, Vol. 5, p. 228.
21. W. L. Chen, A. G. Striz, and C. W. Bert, A new approach to the differential quadrature method for Fourth–Order equations, *Int. J. Num. Methods Eng.* **40**, 1941 (1997).